PREDICTION OF CAFFEINE IN TABLETS CONTAINING ACETYLSALICYLIC ACID, DIPYRONE, AND PARACETAMOL BY NEAR INFRARED SPECTROSCOPY, RAMAN SCATTERING, AND PARTIAL LEAST SQUARES REGRESSION

L. L. M. Guio [1], L. O. Coutinho [1], V. Cavalcante [2], A. Ferreira [3], Z. B. Amorim [1], J. S. Ribeiro [1*]

[1] Laboratory of Beer, Raw Materials and Essential Oils Analysis, Federal Institute of Espirito Santo – Campus Vila Velha, CEP. 29106-010, Brazil; e-mail: julianoribeiro@ifes.edu.br
[2] Metrohm Brazil Analytical Instrumentation, CEP. 05007-030, Sao Paolo, Brazil
[3] Genetics and Breending Laboratory, Federal University of Espirito Santo – Campus Alegre, CEP. 29500-000, Brazil

Two chemometric models drawing on diffuse reflectance near infrared spectroscopy and Raman scattering are proposed to predict caffeine content in tablets based on acetylsalicylic acid, dipyrone, and paracetamol contents. However, data mining from these analyses to create models generally requires a prior comparison between spectral data and the results from reference values obtained by analytical methodology. Therefore, the construction of a robust calibration model entails that both analytical methods are simultaneously employed on several samples, which represents a limiting factor for the widespread use of spectroscopy. In this case, grounded tablets of different brands, containing only the active principles acetylsalicylic acid, dipyrone, or paracetamol and their excipients, were doped with controlled amounts of pure caffeine ranging from 0 to 10%(w/w) and used as calibration samples. Thus, caffeine quantification with a reference method was not necessary. The prediction samples had at least one of the aforementioned active ingredients and caffeine in its original formulation. Hence, the %(w/w) values of caffeine used as reference for the prediction steps were calculated from the values described on the drug description leaflet and the tablet final mass. Partial least squares regression was used as a multivariate method to construct the models. The near infrared and Raman prediction models for caffeine, using four latent variables, presented the respective values of 0.79 and 0.78 of root mean square errors of cross validation, 0.74 and 1.00 of root mean square errors of prediction, and 0.97 and 0.97 of correlation coefficients.

Keywords: *caffeine, acetylsalicylic acid, dipyrone, paracetamol, partial least squares regression, near infrared spectroscopy, Raman scattering.*

ПРОГНОЗИРОВАНИЕ НАЛИЧИЯ КОФЕИНА В ТАБЛЕТКАХ, СОДЕРЖАЩИХ АЦЕТИЛСАЛИЦИЛОВУЮ КИСЛОТУ, ДИПИРОН И ПАРАЦЕТАМОЛ, С ПОМОЩЬЮ СПЕКТРОВ БЛИЖНЕГО ИК-ДИАПАЗОНА, КОМБИНАЦИОННОГО РАССЕЯНИЯ И МЕТОДА ЧАСТИЧНОЙ РЕГРЕССИИ НАИМЕНЬШИХ КВАДРАТОВ

L. L. M. Guio [1], L. O. Coutinho [1], V. Cavalcante [2], A. Ferreira [3], Z. B. Amorim [1], J. S. Ribeiro [1*]

УДК 535.34;535.375.5

[1] Федеральный институт Эспириту-Санту – Кампус Вила-Велья, CEP. 29106-010, Бразилия e-mail: julianoribeiro@ifes.edu.br
[2] Центр аналитического оборудования Metrohm, Бразилия, Сан-Паулу, CEP. 05007-030, Бразилия
[3] Федеральный университет Эспириту-Санту – Кампус Алегри, CEP. 29500-000, Бразилия

(Поступила 16 июля 2020)

Две хемометрические модели, основанные на спектроскопии диффузного отражения в ближней инфракрасной области и комбинационного рассеяния света, предлагаются для прогнозирования

наличия кофеина в таблетках, содержащих ацетилсалициловую кислоту, дипирон и парацетамол. Для создания моделей обычно требуется предварительное сравнение спектральных данных и эталонных значений, полученных с помощью аналитической методологии. Для построения надежной калибровочной модели необходимо одновременное применение обоих аналитических методов на нескольких образцах, что является ограничивающим фактором для широкого использования спектроскопии. Измельченные таблетки различных марок, содержащие только действующие вещества – ацетилсалициловую кислоту, дипирон или парацетамол – и вспомогательные вещества, допировали контролируемым количеством чистого кофеина в диапазоне 0–10 мас.% и использовали в качестве калибровочных образцов. Таким образом, количественного определения кофеина эталонным методом не потребовалось. Образцы для прогнозов содержали по крайней мере один из вышеупомянутых активных ингредиентов и кофеин. Концентрации кофеина (мас.%), используемые в качестве эталонов для этапов прогнозирования, рассчитаны на основе значений, представленных в описании лекарственного средства, и конечной массы таблетки. Регрессия частичных наименьших квадратов использовалась как многомерный метод для построения моделей. Модели прогнозирования, основанные на ближней ИК-спектроскопии и комбинационном рассеянии света, с использованием четырех латентных переменных для кофеина показали следующие результаты: среднеквадратичные ошибки перекрестной проверки 0.79 и 0.78, среднеквадратичные ошибки прогноза 0.74 и 1.00, коэффициенты корреляции 0.97 и 0.97.

Ключевые слова: *кофеин, ацетилсалициловая кислота, дипирон, парацетамол, частичная регрессия наименьших квадратов, ближняя инфракрасная спектроскопия, комбинационное рассеяние.*

Introduction. The worldwide consumption of caffeine (1,3,7-trimethylxanthine), a legal psychostimulant molecule, is considered extremely elevated nowadays, since this molecule can be found in several widely consumed beverages, such as coffee and teas, as well as in a diverse variety of foods, capsules, pills, solutions, meal supplements, and medicines [1, 2]. This substance can be considered one of the most controversial molecules found in nature. Depending on its dosage and due to its varied pharmacological action, caffeine can cause both beneficial (relief of postoperative pain and headache, appetite suppression, and enhancement of cognitive performance) [3] and adverse effects (e.g., nervousness, dizziness, withdrawal syndrome, and tachycardia) [4]. This molecule also acts as a stimulant of both central nervous system [5] and cardiovascular system, also triggering calcium homeostasis [6, 7]. The most frequent appearance of caffeine in medications occurs in painkillers, for the treatment of tension headaches, post-surgical pain, migraines, fibromyalgia [8–11]. The following painkillers can be highlighted: acetylsalicylic acid [12, 13], dipyrone [14–16], paracetamol [17], diclofenac [18], and ibuprofen [19, 20].

In Brazil, the number of people who self-medicate with these painkillers has increased considerably through time due to the ease in acquiring these medicines, which can be sold without a prescription. Therefore, the National Health Surveillance Agency (In Portuguese – Agência Nacional de Vigilância Sanitária– ANVISA) limits the maximum amount of caffeine that could be added into these medicines and dietary supplements [21]. The chief methods described in the scientific literature for the quantification of caffeine in different matrices are high-performance liquid chromatography (HPLC) and its variations [22–25]. Although these chromatographic methods are suitable for the determination of this molecule, these techniques have several negative factors, such as high cost, long analysis time, use of ultrapure solvents, and sample preparation, when compared to certain spectroscopic methods combined with chemometrics [26–29]. The spectroscopic techniques based on near infrared (NIR) and Raman scattering, associated with chemometric tools have appeared to be excellent alternative techniques to quantify compounds, since almost no sample opening and reduced analysis time enhance their efficiency [30–35].

Therefore, this work aims to use near infrared and Raman scattering data with partial least squares regression (PLSR) to predict caffeine content in several commercial ground tablets based mainly on acetylsalicylic acid, dipyrone, and paracetamol. To do this, several other drug samples containing these three active ingredients (acetylsalicylic acid, dipyrone, and paracetamol) and their excipients were doped with pure caffeine (in different percentages) and used to create the two multivariate models. Furthermore, this work also presents an interesting discussion on the selected spectral regions from both spectroscopic techniques to predict caffeine content in complex matrices.

Experimental. Caffeine anhydrous (minimum 99 % purity) was obtained from Sigma–Aldrich (Munich). For the construction of the two calibration sets, tablets containing only acetylsalicylic acid (ASA), dipyrone (DIP), or paracetamol (PARA) with their different excipients were acquired in pharmacies from Vila Velha

City (ES, BR) (2018/2019–2019/2020 batches). For the Raman analyses (2018/2019 batch), four different brands of manufactured tablets (2 for ASA, 1 for DIP and PARA) were acquired (EMS, Neoquímica, Medley and Prati). For the NIR analyses (2019/2020 batch), six different brands of manufactured tablets (two for each active principle) were obtained (Neoquímica, Prati, EMS, Sanofi, Anador and Medley). In both cases, the excipient used in each manufactured tablet could be different (this is important to predict the power of the two multivariate models). It is noteworthy that the Raman data analyses were performed between 2018 and 2019, while the NIR data was acquired between 2019 and 2020. Therefore, the two calibration sets were measured with completely different batches of tablets. For the two prediction sets (NIR and Raman), other manufactured tablets were acquired from novel brands containing a mixture of caffeine and at least one of the active principles (ASA, DIP, and PARA) in their manufactory formulation (nine commercial samples for Raman analyzes 2018–2019 batch, and eight for NIR 2019–2020 batch).

The caffeine concentrations %(w/w) used for the prediction sets were calculated using the mass described on the drug description leaflet and the tablet mass. Hence, it was a nominal value, which was not measured by reference methods, such as HPLC. For the creation of two calibration sets, six tablets per batch were weighed %(w/w), ground, and doped with different caffeine contents (0, 2, 4, 6, 8, and 10%). Thus, a total of 36 and 24 calibration samples containing caffeine between 0 to 10%(w/w) was created for NIR and Raman models, respectively. Diffuse reflectance near-infrared spectra of pure caffeine, ground tablets (containing only ASA, DIP or PAR, and their excipients) as well as all ground and mixed calibration (36) and prediction (8) samples, were obtained using a near infrared Qinterline model DairyQuant FT-NIR. Each spectrum was profiled from 32 scans within the 1100–2500 nm range and a 4 nm resolution. Three spectra were recorded for each sample.

Raman scattering spectra of pure caffeine, ground tablets (containing only ASA, DIP or PAR and their excipients), as well as all grounded and mixed calibration (24) and prediction (9) samples, were obtained using a Metrohm Instant Raman Analyzer (MIRA), with laser wavelength in 785 nm, resolution of 8 cm^{-1}, and spectral range from 400 to 2300 cm^{-1}. Three spectra were recorded for each individual sample.

Chemometric data treatment. The two original spectroscopic profiles were organized into matrix format X_{nir} ($I \times J$), X_{Raman} ($N \times M$), where each replicate was considered as one sample. Data analyses were carried out using Matlab v.2017 software (The MathWorks, Co., Natick, MA, USA) with the PLS Toolbox computational package (Eigenvector Research, Inc. – PLS_Toolbox version 8.61.) [36]. Two pretreatments were applied to both original data matrices (X_{nir}, X_{Raman}): (i) Savitzky–Golay smoothing with a window size of 7 and 11 points, respectively, and (ii) first derivative [37]. The partial least squares method (PLS) was used as a regression method for modeling [38]. Variable selection was carried out by the ordered predictors selection method (OPS) [39] and followed by visual inspection with the aid of pure spectra of caffeine and the spectra of ground tablets (containing only ASA, DIP or PAR and their excipients).

Results and discussion. *PLS model with NIR data***.** The original NIR spectra of all calibration samples and the ground tablets of prediction samples were organized into a format X_{nir} matrix (132×661) containing 132 replicates (I) and 661 wavelengths (J). Figure 1 shows both original and pretreated spectra (X_{p1}).

For the development of the regression model to predict caffeine contents %(w/w), the dependent variables (y) used for calibration samples ranged from 0 to 10 %(w/w), while the prediction samples were calculated using the ratio between caffeine mass, indicated on the drug description leaflet, and the total mass of each tablet (nominal values). The pretreated NIR spectra (X_{p1}) were established as independent variables.

The data set was split as follows: 36 samples (108 spectra) were used as calibration set, while eight different external samples, corresponding to 24 spectra, were utilized for external validation. Leave-five-out cross-validation was the method used to select the number of latent variables in the model (15 replicates of five samples were withdrawn and calculated at a time).

From the initial 661 variables, the OPS algorithm and the visual selection identified 17 regions (100 wavelengths) to build the PLS-NIR model, as shown by the vertical lines in Fig. 2.

Table 1 displays the regions defined by the variables selected for the calibration model as well as the corresponding vibrational modes and charts. Considering the first row of Table 1, the variables ranging from 1138 to 1142 were selected for the calibration model and were related to the 3rd and 2nd overtones of the CH or CH_3 charts.

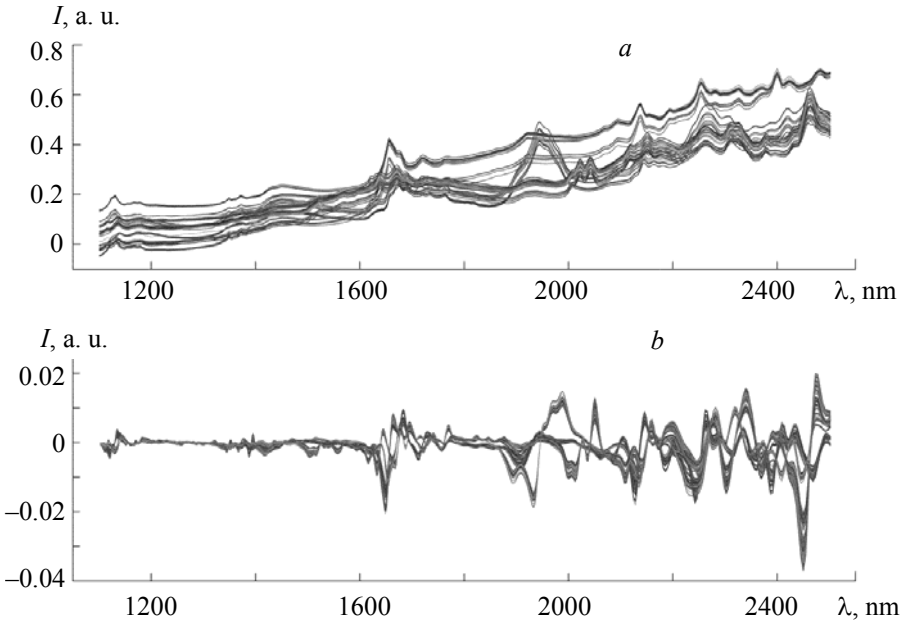

Fig. 1. Original (a) and pretreated (b) diffuse reflectance near-infrared spectra of all samples.

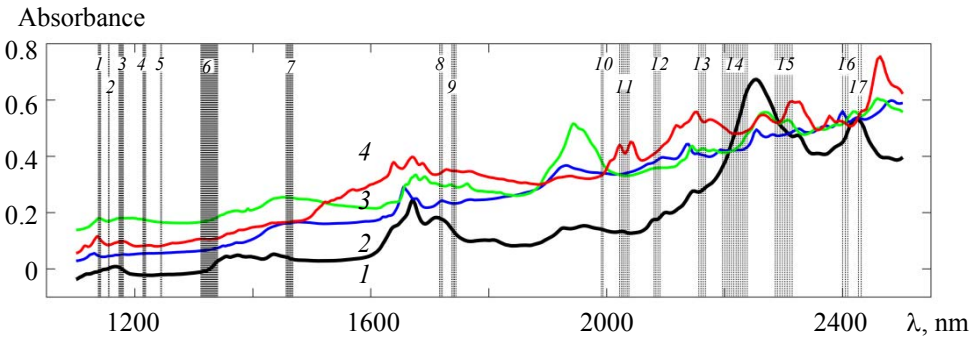

Fig. 2. Selected variables for the PLS caffeine prediction model using NIR data. The spectra are from pure caffeine (1), ASA (2), DIP (3), and PARA (4) ground tablets.

TABLE 1. Regions Selected by OPS to Construct the PLS Model with NIR Data

Regions selected	General ranges, nm	Vibrational modes	Charts
1	1138–1142*	3rd and 2nd overtone of C–H	CH_3
2	1155–1157*	2nd overtone of C–H	CH_3 and CH_2
3	1173–1181*	2nd overtone of C–H	CH and CH_2
4	1213–1218	2nd overtone of C–H	CH
5	1244–1245	2nd overtone of C–H	–
6	1312–1340*	2nd overtone of C–H	–
7	1456–1468*	2nd overtone of O–H, C–H, N–H	C–H, $CONH_2$, ROH
8	1716–1721*	1st overtone of C–H	CH, CH_2, CH_3
9	1736–1745*	1st overtone of C–H	CH, CH_2, SH_3
10	1991–1994	1st overtone of C–H and combination bands	–
11	2022–2038	1st overtone of C O and O–H combination bands	–
12	2080–2090	O–H combination bands	ROH, $CONH_2$(R)
13	2155–2168	N–H, O–H and C-C combination bands	–
14	2196–2239*	N–H, O–H and C-C combination bands	CH_3, CC, CHO, RNH_2

Continue Table 1

Regions selected	General ranges, nm	Vibrational modes	Charts
15	2286–2315*	C–H + C–H and C – H + C-C combination bands	H_2O, CH, CH_2, CH_3
16	2400–2410	C–H + C–H combination bands	CH, CH_2, CH_3
17	2426–2432*	C–H + C–H combination bands	CH and CH_2

* Regions selected as pure caffeine [40].

TABLE 2. Calculated and Predicted Caffeine Contents from the PLS Model with NIR Data

Prediction samples	Calculated %(w/w)*	Predicted %(w/w)**
S_{NIR1} (ASA + caffeine)	7.70	6.60 ± 0.10
S_{NIR2} (ASA + caffeine)	9.96	10.51 ± 0.66
S_{NIR3} (ASA + caffeine)	9.87	10.01 ± 0.23
S_{NIR4} (DIP + caffeine)	5.11	5.46 ± 0.25
S_{NIR5} (DIP + caffeine)	9.99	9.63 ± 0.05
S_{NIR6} (DIP + caffeine)	4.78	5.68 ± 0.23
S_{NIR7} (PARA + caffeine)	8.50	8.90 ± 0.15
S_{NIR8} (PARA + caffeine)	8.30	7.36 ± 0.20

*Using the mass described on the drug description leaflet and the measured mass of the entire tablets.
**Standard deviation between replicates.

The number of latent variables used in this PLS model was determined by the root mean square error of cross validation (RMSECV) values. The four latent variables (4 LV) could explain 95.32 and 98.23% of the variance used in blocks Y and X, respectively. So, the calculated PLS model presented a RMSECV of 0.79 and a cross validation correlation coefficient (r_{vc}) of 0.97. The model was validated by the external data set indicated in Table 2, and the root mean square error of prediction (RMSEP) was 0.74. Table 2 also shows the calculated and predicted values of the prediction samples for the PLS model.

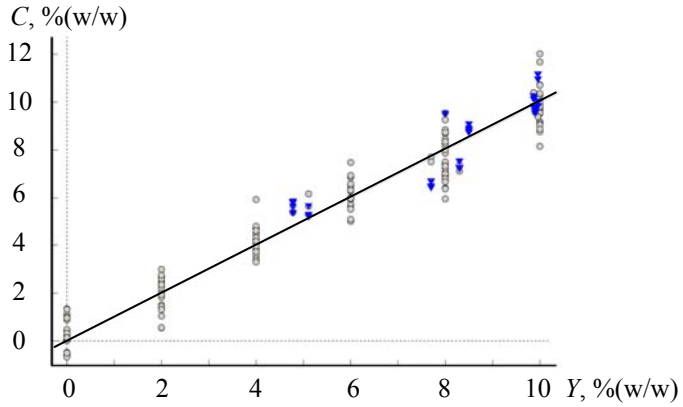

Fig. 3. Calculated *vs*. predicted values of caffeine contents for the calibration (o) and prediction (▲) sets in the PLS model using NIR data

Figure 3 presents the calculated values for caffeine %(w/w) and the respective values estimated from the cross-validation step constructed with NIR data. The predicted values for the external validation samples were also included. In general, articles describing the use of NIR to determine dipyrone [14], paracetamol [41, 42], and acetylsalicylic acid [12] hardly mention the main absorption bands of these compounds, but certain studies pointed out the entire regions for caffeine (1560–2500 nm), paracetamol (1110–2500 nm) [32], dipyrone (1100–1250, 1250–1550; 1650, 1675, 1934, and 2139 nm) [43, 15], and acetylsalicylic acid (1587–1695 nm) [44].

Thus, the NIR spectra of pure caffeine was plotted together with the spectra of ASA, DIP, and PARA ground tablets (Fig. 2) to identify and understand the wavelengths that can validate the PLS model.

Ten of the seventeen selected bands, presented in Table 1 (1, 2, 3, 6, 7, 8, 9, 14, 15, and 17), appear to be from pure caffeine spectra in Fig. 2. All these caffeine bands are also listed in the work of Ribeiro et al. [40]. These results have shown that the built model has several regions of caffeine absorption, thus enhancing accuracy and reliability of the predictions.

PLS model with Raman scattering data. The original Raman spectra of almost all calibration samples and the ground tablets for caffeine prediction were organized into a matrix format, X_{Raman} (99×1901). The matrix contained 99 replicates (N) and 1901 wavenumber (M, cm^{-1}). Figure 4 portrays the original and the pretreated Raman spectra (X_{p2}).

The PLS model development to predict caffeine content with Raman data followed a similar trend to the model with NIR data, where the dependent variables (y) used for (i) calibration samples ranged from 0 to 10 %(w/w) (doped samples), while the ratio between the caffeine mass on the drug description leaflet and the total mass of each table was utilized for the (ii) prediction samples. The pretreated Raman spectra (matrix X_{p2}) were employed as independent variables.

The data set was split as follows: 24 samples (72 spectra) were used as a calibration set, and nine external samples, corresponding to 27 spectra, were used for external validation. Leave–five-out cross-validation was the method used to select the number of latent variables in the model (15 replicates of five samples were withdrawn and calculated at a time).

From the initial 1901 variables, the OPS algorithm followed by the visual selection identified 11 regions (150 wavenumbers) to build the PLS model as indicated by the vertical lines in Fig. 5.

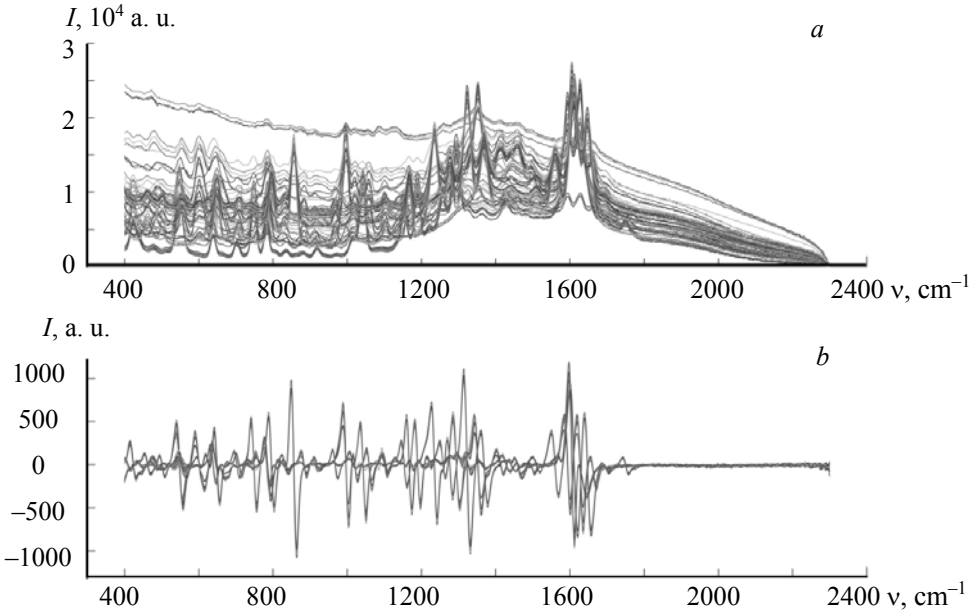

Fig. 4. Original (a) and pretreated (b) spectra of almost all samples analyzed by Raman scattering.

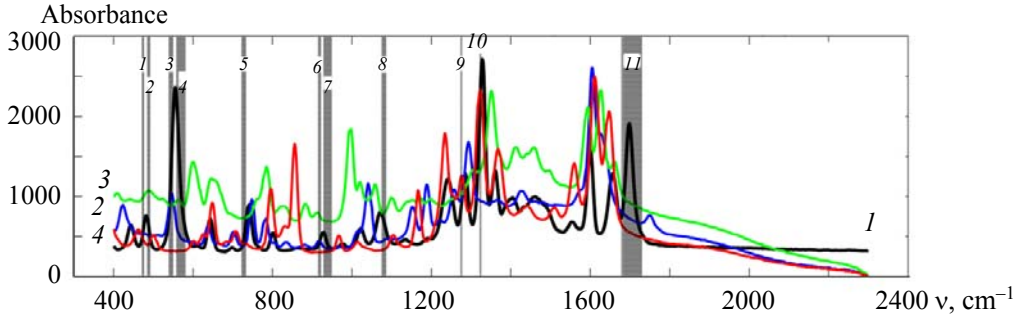

Fig. 5. Selected variables for the PLS caffeine prediction model using Raman scattering data. The spectra are from pure caffeine (1), ASA (2), DIP (3), and PARA (4) ground tablets.

The Raman scattering spectra, from 400 to 2300 cm^{-1}, of pure caffeine and ground tablets containing either ASA, DIP or PARA are shown in Fig. 5. The wavenumbers of the 11 bands selected from the Raman spectra for the calibration model can be seen in Table 3. Vibrational assignments are provided for pure caffeine spectra from [45, 46] and Fig. 5.

TABLE 3. Regions Selected by OPS for the Construction of the Raman PLS Model

Regions selected	Wavenumber, cm^{-1}	Vibrational assignments
1	473–476, *m*	δ(pyrimidine ring) + δ(CNO) + δ(CH)
2	485–492, *m*	δ(pyrimidine ring) + δ(CNO) + δ(CH)
3	540–550, *s*	δ(pyrimidine ring) + δ(CNC) + ρ(CH_3)
4	559–579, *s*	δ(pyrimidine ring) + δ(CNC) + ρ(CH_3)
5	723–733, *m*	δ(pyrimidine, imidazole ring) + δ(CH_3) + ρ(CH_3)
6	916–921, *w*	ρ(CH_3)
7	930–947, *w*	ρ(CH_3)
8	1076–1085, *m*	δ(CH–N)
9	1274–1275, *m*	ν(C–N) + ρ(CH_3)
10	1322–1324, *s*	ν(imidazole ring)
11	1679–1729, *s*	ν(C=O) in phase

N o t e. δ, Deformation; ν, stretching; ρ, bending; *s*, strong; *m*, medium; *w*, weak.

The PLS model with Raman scattering data was also constructed with four latent variables (4 LV), using RMSECV values as parameters. These 4 LV could explain 95.19 and 97.44% of the variance used in blocks Y and X, respectively. The model presented a RMSECV of 0.78 and a cross-validation correlation coefficient (r_{vc}) of 0.97 and was validated by the external data set (Table 4) with RMSEP of 1.00. Table 4 also shows the calculated and predicted values of the prediction samples for the PLS-Raman model.

Figure 6 shows the calculated values for caffeine %(w/w) and the respective values estimated from the cross-validation step constructed with Raman scattering data. The predicted values for the external validation samples were also included to highlight their values within the range of the calibration samples.

TABLE 4. Calculated and Predicted Caffeine Contents from the PLS-Raman Regression Model

Prediction samples	Calculated %(w/w)*	Predicted caffeine contents %(w/w)**
S_{R1} (DIP + dexclopheniramine maleate + caffeine)	4.42	3.57 ± 0.00
S_{R2} (ASA + caffeine)	7.65	6.45 ± 1.08
S_{R3} (DIP + caffeine)	9.92	11.51 ± 0.62
S_{R4} (ASA + Phenylephrine + caffeine)	4.43	3.19 ± 0.36
S_{R5} (DIP + orphenandrine citrate + caffeine)	7.40	6.20 ± 0.12
S_{R6} (ASA + caffeine)	5.00	5.91 ± 0.38
S_{R7} (ASA + caffeine)	4.90	5.31 ± 0.40
S_{R8} (DIP + orphenandrine citrate + caffeine)	7.71	7.77 ± 0.67
S_{R9} (PARA + diclofenac + carisoprodol + caffeine)	3.77	3.79 ± 0.51

*Using the mass described on the drug description leaflet and the measured mass of the entire tablets. **Standard deviation between triplicates.

At this moment, a discussion on the spectral bands used by the PLS-Raman model to predict caffeine contents is necessary. Two previous works on Raman spectrum of caffeine assisted on the interpretation of the main spreading bands. Pavel et al. [45] studied both theoretical and pH dependent surface enhanced Raman spectroscopy of caffeine, while Edwards et al. [46] focused on the characterization and discrimination between caffeine, theobromine, and theophylline by Raman spectroscopy. In both works, complete tables of the pure caffeine bands and its vibrational assignments are presented.

According to these tables [45, 46] and the pure spectra of caffeine in Fig. 5, it could be verified that the 11 spectroscopic bands listed in Table 3 correspond to caffeine and, therefore, the mathematical model described here has elevated predictive power.

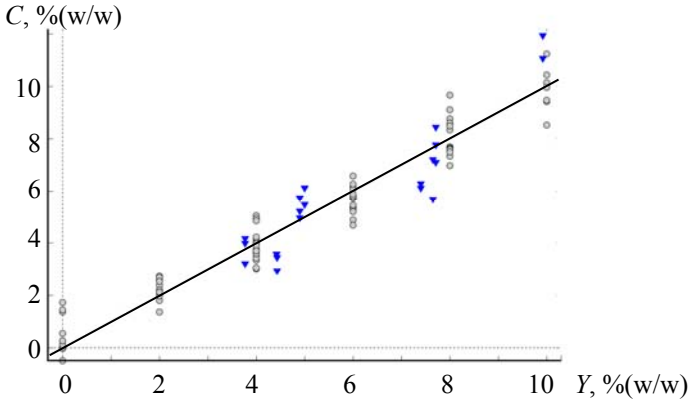

Fig. 6. Calculated *vs*. predicted values of caffeine contents for the calibration (○) and prediction (▲) sets in the PLS model using Raman scattering data.

Conclusions. Although the two partial least square models were not performed with the same batches of samples (2018/2019 and 2019/2020), the strategy of doping different ground tablets with caffeine contents in the calibration step proved to be promising for further prediction of commercial samples. The predictive power of the two partial least square models also demonstrated the importance of the variable selection step, since the matrices were noticeably complex (models built with acetylsalicylic acid, dipyrone, paracetamol, and different excipients). Comparison of the selected variables with the pure caffeine spectra demonstrated that practically all regions selected for near infrared and Raman models were strictly linked to the desired molecule. Even though a significant difference between the quality of the two models was expected, since one of them was constructed in a bench equipment and had a higher resolution compared to the other portable one, both presented practically identical outcomes (RMSECV, RMSEP and r_{cv}).

Acknowledgments. This study was partially funded by the Fundação de Amparo à Pesquisa e Inovação do Espírito Santo (FAPES). The authors are grateful to Ramon Azevedo Braz, Mayra Neres da Silva, Amanda Moura Dutra, Sofia Soares do Nascimento, and Yasmin Dilkin, who contributed to improve the quality of this work.

REFERENCES

1. J. L. Temple, C. Bernard, S. E. Lipshultz, J. D. Czachor, J. A. Westphal, M. A. Mestre, *Front. Psy*., **8**, 1–19 (2017).
2. M. C. Cornelis, *Nutrients*, **11**, 416–420 (2019).
3. A. Shabir, A. Hooton, J. Tallis, M. Higgins, *Nutrients*, **10**, 1528 (2018).
4. D. Wikoff, B. T. Welsh, R. Henderson, G. P. Brorby, J. Britt, E. Myers, J. Goldberger, H. R. Lieberman, C. O'Brien, J. Peck, M. Tenebein, C. Weaver, S. Harvey, J. Urban, C. Doepker, *Food Chem. Toxicol.*, **109**, 585–648 (2017).
5. A. Nehlig, J. Daval, G. Debry, *Brain Res. Rev.*, **17**, 139–170 (1992).
6. J. Sawynok, *Pain*, **152**, 726–729 (2011).
7. R. P. Heaney, *Food Chem. Toxicol*., **40**, 1263–1270 (2002).
8. A. R. Feinstein, L. Heinemann, D. Dalessio, J. M. Fox, J. Goldstein, G. Haag, D. Ladewig, C. P. O'Brien, *Clin. Pharmacol. Ther*., **68**, 457–467 (2000).
9. H. R. V. Godoy, F. B. Gonçalves, C. F. Moraes, *Rev. Med. Saude*, **1**, 169–173 (2012).
10. V. A. Voicu, C. Mircioiu, C. Plesa, M. Jinga, V. Balaban, R. Sandulovici, A. M. Costache, V. Anuta, I. Mircioiu, *Front. Pharmacol*., **10**, 607 (2019).
11. J. R. Scott, A. L. Hassett, C. M. Brummett, R. E. Harris, D. J. Clauw, S. E. Harte, *J. Pain Res*., **10**, 1801–1809 (2017).
12. J. Cruz, M. Bautista, J. M. Amigo, M. Blanco, *Talanta*, **80**, 473–478 (2009).
13. E. M. Aldred, *Pharmacology, a Handbook for Complementary Healthcare Professionals*, 41, 331–341 (2009).
14. F. A. C. Sanches, R. B. Abreua, M. J. C. Pontes, F. C. Leite, D. J. E. Costa, R. K. H. Galvão, M. C. U. Araujo, *Talanta*, **92**, 84–86 (2012).

15. C. A. D. Melo, P. Silva, A. A. Gomes, D. D. S. Fernandes, G. Véras, A. C. D. Medeiros, *J. Braz. Chem. Soc*., **24**, 991–997 (2013).
16. M. I. Díaz-Reval, R. Galván-Orozco, F. J. López-Muñoz, N. Carrillo-Munguía, *Cir. Ciruj*., **76**, 241–246 (2008).
17. G. G. Graham, M. J. Davies, R. O. Day, A. M. K. F. Scott, *Inflammopharmacology*, **21**, 201–232 (2013).
18. S. J. Peroutka, J. A. Lyon, J. Swarbrick, R. B. Lipton, K. Kolodner, J. Goldstein, *Headache*, **44**, 136–141 (2004).
19. S. Diamond, T. K. Balm, F. G. Freitag, *Clin. Pharmacol. Ther*., **68**, 312–319 (2000).
20. A. Polski, R. Kasperek, K. Sobotka-Polska, E. Poleszak, *Curr. Issues Pharm. Med. Sci.*, **27**, 10–13 (2014).
21. http://portal.anvisa.gov.br/documents/3845226/0/Justificativa_Limites_Suplementos.pdf/e265ccd0-8361-4d8e-a33f-ce8b2ca69424.
22. S. C. Escobar, L. R. Cubides, C. P. Pérez, *Indian J. Pharm. Sci*., **79**, 731–739 (2017).
23. R. C. Lopez-Sanchez, V. J. Lara-Diaz, A. Aranda-Gutierrez, J. A. Martinez-Cardona, J. A. Hernandez, *J. Anal. Methods Chem*., **2018**, 1–11 (2018).
24. M. F. F. Lima, G. I. S. França, D. J. F. Souza, A. G. S. Cabral, C. A. de Azevedo Filho, *Braz. J. Health Rev*., **2**, 4600–4610 (2019).
25. M. Jeszka-Skowron, A. Zgoła-Grzeskowiak, T. Grzeskowiak, *Eur. Food Res. Technol*., **240**, 19–31 (2015).
26. M. C. Sarraguça, A. V. Cruz, S. O. Soares, H. R. Amaral, P. C. Costa, J. A. Lopes, *J. Pharm. Biomed. Anal*., **52**, 484–492 (2010).
27. D. Melucci, D. Monti, M. D'Elia, G. Luciano, *J. Forensic Sci*., **57**, 86–92 (2012).
28. Y. Sacré, F. Chavez, L. Netchacovicth, Ph. Hubert, E. Ziemos, *J. Pham. Biomed. Anal.*, **101**, 123–140 (2014).
29. C. S. Silva, A. Braz, M. F. Pimentel, *J. Braz. Chem. Soc*., **30**, 2259–2290 (2019).
30. A. B. Eldin, O. A. Ismaiel, W. E. Hassan, A. A. Shalaby, *J. Anal. Chem*., **71**, 861–871 (2016).
31. M. Palo, K. Kogermann, N. Genina, D. Fors, J. Peltonen, J. Heinämäki, N. Sandler, *J. Drug Deliv. Sci. Technol*., **34**, 60–70 (2015).
32. D. M. Muntean, C. Alecu, I. Tomuta, *J. Spectrosc*., **2017**, 1–8 (2017).
33. Y. Roggo, K. Degardina, P. Margot, *Talanta*, **81**, 988–995 (2010).
34. N. M. Ralbovsky, I. K. Lednev, *Spectrochim. Acta A*, **219**, 463–487 (2019).
35. B. Nagy, A. Farkas, M. Gyurkes, S. Komaromy-Hiller, B. Demuth, B. Szabo, D. Nusser, E. Borbas, G. Marosi, Z. Kristof, *Int. J. Pharm*., **530**, 21–29 (2017).
36. B. M. Wise, N. B. Gallagher, R. Bro, J. M. Shaver, W. Windig, R. S. Koch, *PLS_Toolbox 3.5, for Use with MatlabTM*, Eigenvector Research (2004).
37. A. Savitzky, M. J. E. Golay, *Anal. Chem*., **36**, 1627–1679 (1964).
38. R. G. Brereton, *Applied Chemometrics for Scientists*, John Wiley & Sons (2007).
39. J. V. Roque, W. Cardoso, L. A. Peternelli, R. F. Teófilo, *Anal. Chim. Acta*, **1075**, 57–70 (2019).
40. J. S. Ribeiro, M. M. C. Ferreira, T. J. G. Salva, *Talanta*, **83**, 1352–1358 (2011).
41. M. M. Said, S. Gibbons, A. C. Moffata, M. Zloha, *Int. J. Pharm*., **415**, 102–109 (2011).
42. M. Blanco, R. Cueva-Mestanza, A. Peguero, *J. Pharm. Biomed. Anal*., **51**, 797–804 (2010).
43. M. H. Ferreira, J. F. F. Gomes, M. M. Sena, *J. Braz. Chem. Soc*., **20**, 1680–1686 (2009).
44. E. Otsuka, H. Abe, M. Aburada, *Drug Dev. Ind. Pharm*., **36**, 839–844 (2010).
45. I. Pavel, A. Szeghalmi, D. Moringnio, S. Cinta, W. Kiefer, *Biopolymers*, **72**, 25–37 (2003).
46. H. G. M. Edwards, T. Munshi, M. Anstis, *Spectrochim. Acta A*, **61**, 1453–1459 (2005).